LVRT Enhancement of a Grid-tied PMSG-based Wind Farm using Static VAR Compensator

Shoaib Ahmed Dayo
Department of Electrical Engineering
Mehran University of Engineering and Technology
SZAB Campus, Khairpur Mirs, Pakistan
shoaibahmed-dayo@muetkhp.edu.pk

Shafqat Hussain Memon
Department of Electrical Engineering
Mehran University of Engineering and Technology
SZAB Campus, Khairpur Mirs, Pakistan
shafqatmemon@muetkhp.edu.pk

Mohammad Aslam Uqaili
Department of Electrical Engineering
Mehran University of Engineering and Technology
Jamshoro, Pakistan
aslam.uqaili@faculty.muet.edu.pk

Zubair Ahmed Memon
Department of Electrical Engineering
Mehran University of Engineering and Technology
Jamshoro, Pakistan
zubair.memon@faculty.muet.edu.pk

Abstract-This paper presents an efficient Low Voltage Ride Through (LVRT) control scheme for a 10.0MW grid-tied Permanent Magnet Synchronous Generator (PMSG)-based wind farm. The proposed control strategy plans to enhance the power quality and amount of injected power to satisfy the grid code requirements. The proposed approach utilizes a static Shunt Var Compensator (SVC) to enhance the LVRT capability and to improve power quality. It has been observed from the outcomes of the study that the proposed SVC controller ensures safe and reliable operation of the considered PMSG-based power system. The proposed system not only improves power quality but also it provides voltage stability of the Wind Energy Conversion System (WECS) under abnormal/fault conditions. The results show the superiority of the proposed control strategy.

Keywords-LVRT; PMSG; SVC; WECS; power quality; voltage stability

I. INTRODUCTION

The demand for renewable energy sources that produce clean energy with low carbon footprint is increasing. Fossil fuel consumption emits CO_2 resulting in enhanced environmental pollution. Research and development in the energy sector have boosted the extension of renewable energy resources like wind, hydro, and solar [1, 2]. Wind power generation is one of the most promising contributors to the usage of renewable energy [3, 4]. The wind generation potential integrated with the grid is increasing at an optimal level in electricity production fulfilling the energy gap [5] to an extent. Past studies have considered the disconnections of wind farms from the grid in the case of fault occurrence [6]. However, the use of modern grid codes is a prominent solution that ensures the grid system's operational capability even during the occurrence of faults [6-10]. Among multiple types of wind turbines, Permanent Magnet Synchronous Generators (PMSGs) [11] and Double Fed Induction Generators (DFIGs) are widely used in wind farms [1, 5, 12-14]. Development in semiconductor switching devices and high efficiency demand the extension of the use of PMSGs [5, 8, 14]. Authors in [8] explored the LVRT capability enhancement along with the controlled supply of reactive power. Authors in [2] compared FACTS Static Var Compensator (SVC) controller and STATCOM regarding the provision of faster dynamic response to the wind system to control and enhance the LVRT. The SVC was installed at the end of the transmission line to enhance the LVRT control capability during a fault condition in order to maintain supply continuity. SVC was mostly used when voltage swings were the greatest.

The conventional back-to-back converter control strategy of Rotor Side Converter (RSC) was introduced for Maximum Power Point Tracking (MPPT) [15] and Grid Side Converter (GSC) was implemented to regulate the DC link voltage resulting from the grid fault occurrence [7, 8, 16]. When an LVRT occurs, the DC link voltage can be increased because MSC does not sense the grid fault and GSC fails to control the DC link voltage [5, 6, 17, 18] which results in the tripping of the wind farm. The use of a non-linear, SVC controller is rapidly growing because of its robustness with respect to external disturbances. The prime issue of controllers using traditional back-to-back converters is blathering. To reduce blathering, various LVRT methods have been introduced [1-5, 17-19]. The most attractive LVRT method is the SVC because of shunt connection and longer life cycle [2]. Moreover, many authors have proposed different control techniques to enhance the LVRT capability of wind farms [18]. The SVC controller is robust and cost-effective and can be implemented in wind farms. During fault conditions, SVC is capable of enhancing the LVRT performance by supplying the reactive power and thus improve voltage stability [1, 5, 6, 17]. According to the National Electric Power Regulatory Authority (NEPRA) standard, the wind system must be able to withstand voltage sags of around 30% of rated voltage for durations of 80ms [9].

Corresponding author: Shoaib Ahmed Dayo

In this paper, the conventional SVC controller is employed; the LVRT features have been enhanced and maintain voltage supply continuously. The improvement in the wind farm performance has been analyzed. The proposed model design achieves excellent power quality, optimal voltage stability, and reasonable reactive power compensation. The main contributions of this work are:

- The study provides detailed modeling and analysis of a 10.0MW, 120kV grid-connected PMSG wind farm.
- The SVC controller is employed to compensate for reactive power and to enhance the LVRT capability of the developed PMSG-based wind farm during normal and abnormal conditions.
- The proposed system provides uninterrupted power supply to the grid once the fault is removed, thus validating the effectiveness of the proposed control strategy.

II. System Model and Control Strategy

Figure 1 shows the model layout and the control strategy of the proposed system. The wind farm is designed with 5 wind turbines, each with a rating of 2.0MW. The model design comprises of a PMSG based grid integrated wind farm along with an SVC controller. The 10.0MW wind farm has been integrated to a 120kV grid. The proposed model is designed at 50Hz to validate the performance of the system in LVRT conditions. Further, a variable speed PMSG machine is used because of its cost-effectiveness and high efficiency. During the LVRT condition, an SVC controller is installed at the Point of Common Coupling (PCC) to maintain the supply continuity. The bus voltage at PCC is 575V. As per the NEPRA standard, if a voltage dip occurs, the system must not drop below 30% of the rated voltage. The designed control strategy of the SVC controller comprises of a voltage measurement unit, a regulator, a distribution unit, and a synchronizing unit. The voltage measurement module measures the output voltage of the system. It can also be used for filtering purposes. To achieve a smooth voltage response, the voltage regulator is used to control and regulate the voltage. The distribution unit is used to control the thyristor susceptance module and is interfaced with the power system. It also determines the number of Thyristor Switched Capacitor (TSC) units and the absorption level of Thyristor-Controlled Reactor (TCR) power.

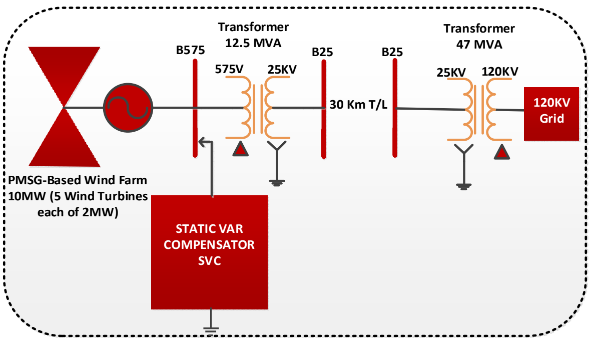

Fig. 1. The PMSG based grid integrated wind farm.

A synchronizing unit contains a Phase-Locked Loop (PLL) circuit which is synchronized against secondary voltages. A pulse generator produces the pulses to energize the thyristors. The SCR starts conducting at a particular point of the voltage known as the firing angle. Lowering the firing angle increases output power. It can be observed that the installation of an SVC controller results in LVRT operation enhancement and as a result, the system performance is improved.

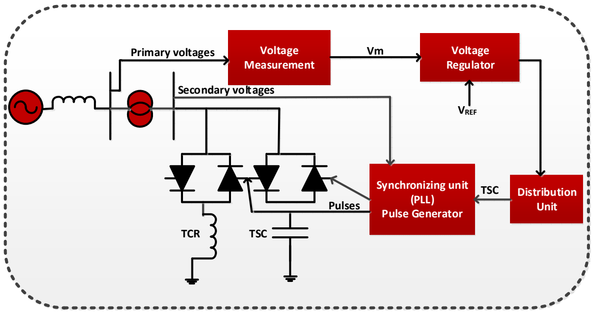

Fig. 2. The designed strategy of the SVC controller.

The result shows the voltage profile is maintained at 0.75p.u. during the LVRT condition. Hence, the continuity of supply is ensured. Power quality and voltage stability during disturbances are also improved. The proposed model was designed and simulated in MATLAB/ Simulink version 2016b. The parameters of the proposed model are listed in Table I.

TABLE I. PROPOSED MODEL SYSTEM PARAMETERS

Parameter name	Value	Parameter name	Value
C_p (max)	11.0	P_n (VA)	2000000/0.9
ρ (K_g/m^3)	1.225	f_n (Hz)	50
ω_m (rad/s)	0.3	R_s (p.u.)	0.006
H (s)	4.32	V_{dc}	1100
Kp	1.1	Ki	27.5
C (nF)	250	L (mH)	1.13
Rs	4.26	Quality factor	50

III. Simulated Results Analysis

In this section, the performance analysis of the proposed system at different stages is evaluated. The steady-state and transient responses during fault conditions, such as SLG and L-L fault, are analyzed in the simulation results. Furthermore, the outcomes of multiple fault conditions on voltage stability and reactive power compensation are also taken into consideration. The Grid-tied PMSG-based wind farm model in MATLAB/Simulink is given in Figure 3. The model consists of a 10MW Wind farm with 1 TCR and 3 TSCs. The rating of TCR is 109Mvar while that of each TSC unit is 94Mvar.

A. System Response at Steady State Condition

This section investigates the operation and control of the proposed model where the voltage is set at 1.0p.u. with generator rating of 5×2MW and V=575V at B575. The active generated power increases steadily and reaches the nominal value of 10MW as shown in Figure 4. The simulation results confirm that the proposed system is running smoothly and shows a good performance during the steady-state condition.

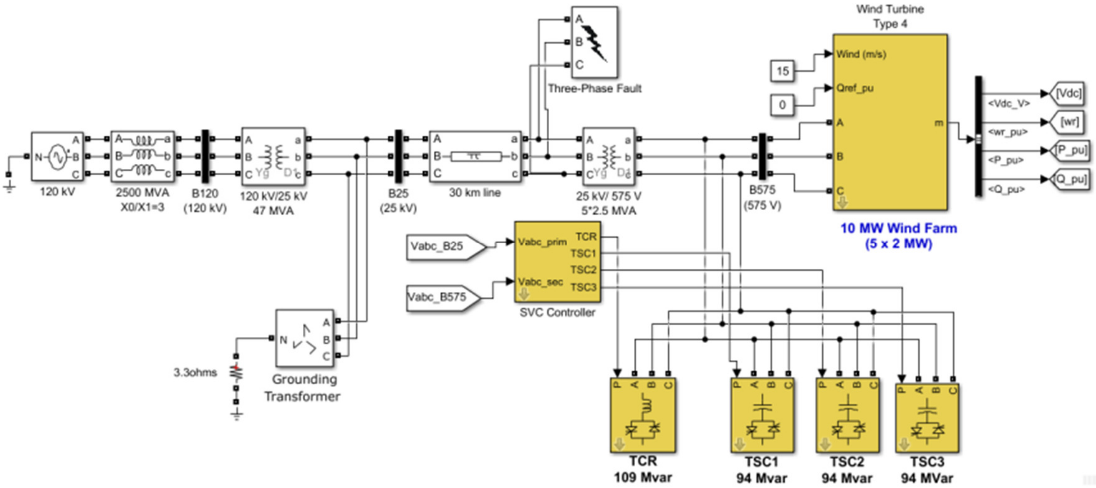

Fig. 3. MATLAB/Simulink model of the proposed system.

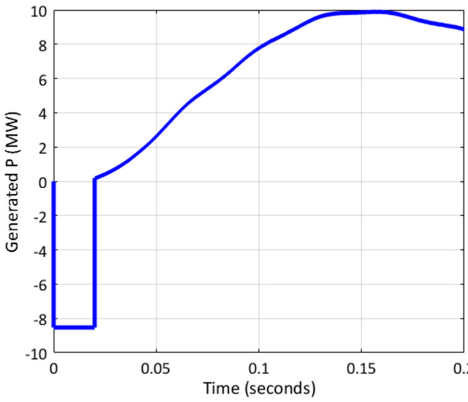

Fig. 4. Active power generation against time.

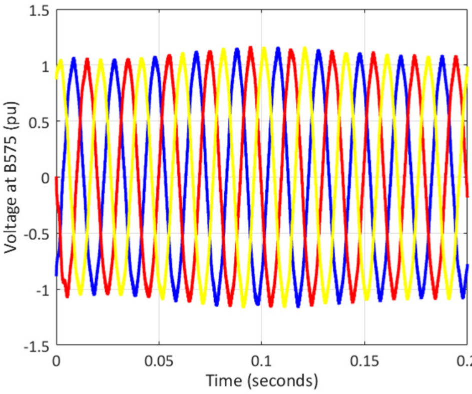

Fig. 5. Voltage response at PCC B575.

The simulation results confirm that the voltage is maintained at 1.0p.u., when the stop time is set at 0.2s. This result is obtained by running iterative rigorous simulations. Figure 5 shows that the optimized value is obtained at 1.0p.u.. During the steady-state condition, the current is not increased beyond the limit. However, from simulation results, it can be seen that the current increases and reaches 0.81p.u. as shown in Figure 5. This shows an excellent performance and proves that the proposed system runs smoothly without any disturbance. The speed turbine starts from 1.0p.u. and reaches up to 1.027p.u. as demonstrated in Figure 6.

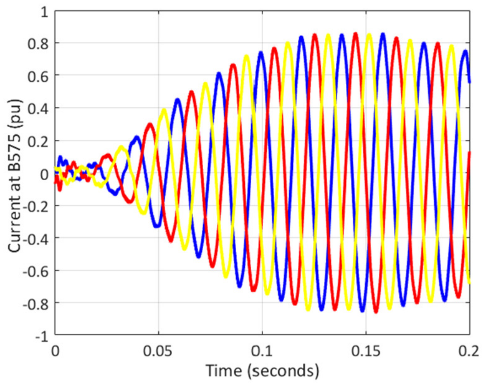

Fig. 6. Generated current at PCC B575.

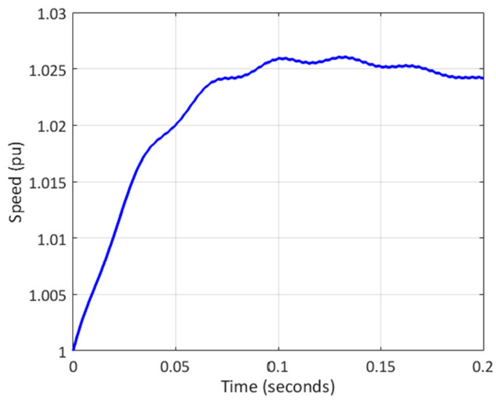

Fig. 7. Turbine speed over the specified time.

It can be observed that the turbine speed is in the safe range and shows the good performance of the proposed system. Figure 8 elucidates the voltage at PCC B575 which is maintained at 1.0p.u. by controlling the amount of reactive power and the wind farm has equivalent dc-link voltage of 1100V. It is increased due to the control process of back-to-back converters in the conventional design.

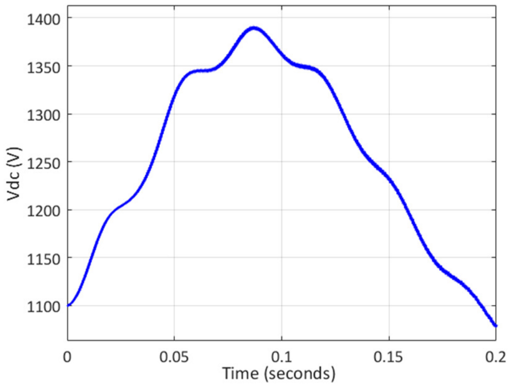

Fig. 8. DC link equivalent voltage across time.

B. System Response at Unsymmetrical SLG Fault

1) Without SVC

The unsymmetrical Single Line to Ground (SLG) fault injected at PCC is demonstrated in Figure 9.

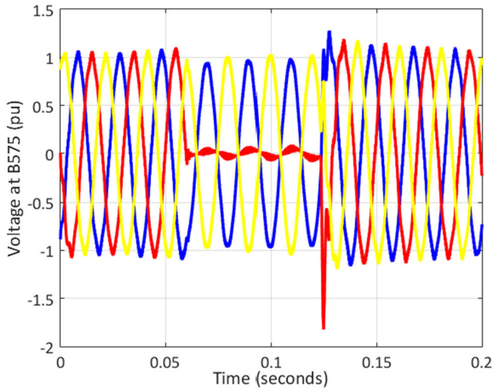

Fig. 9. Generated voltage at PCC B575 during SLG fault.

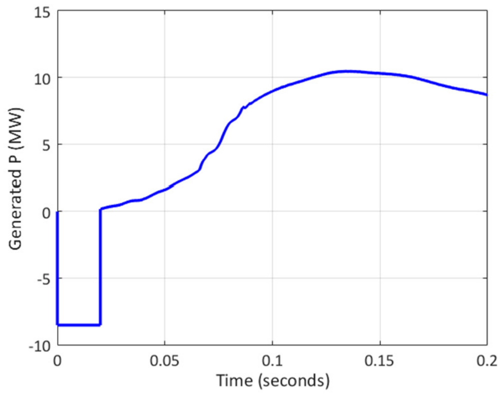

Fig. 10. Generated active power during SLG fault.

One phase is dropped (red line) below 0.5p.u. and the proposed wind farm system is tripped. Hence, the output power of the system becomes zero. Figure 10 shows the variation in the generated power from 0.04 to 0.08s. It can be seen that the optimized 10MW power has certain variations during fault switching time. Further, the variation in the generated power has been observed mainly due to the SLG fault condition. The result also shows the overall performance of the proposed model during temporary injected fault time. During the fault injection, very small reactive power is generated. The reactive power provides some power to run the proposed system model smoothly. Figure 11 shows the poor performance of the system due to the SLG fault.

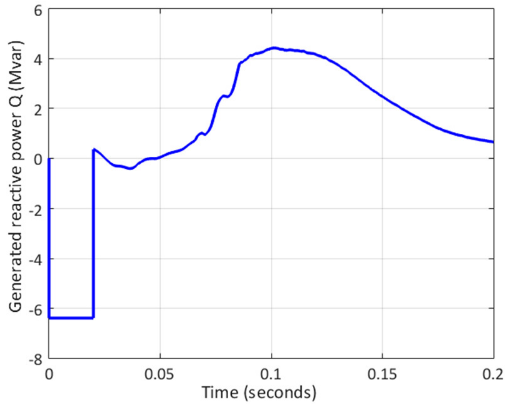

Fig. 11. Generated reactive power during SLG fault.

2) With SVC

Figure 12 shows the bus voltages with an SVC implemented at bus-3 during SLG fault.

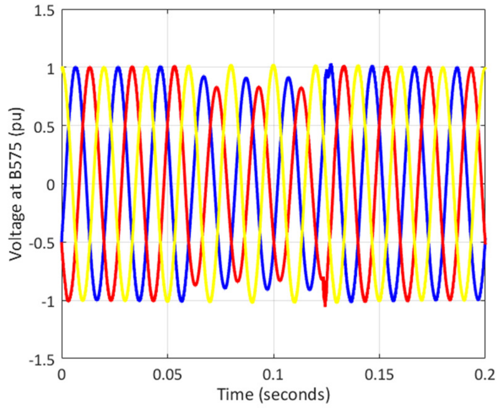

Fig. 12. Voltage at PCC during SLG fault with SVC.

The SVC ensures that the grid integrated wind farm maintains its voltage profile above the value of 0.75p.u.. Therefore, voltage stability and power quality are improved. The wind system continues its connection during fault switching time from 0.06 to 0.12s with the grid by supplying reactive power. The wind farm is not disconnected from the grid and the continuity of supply is maintained. The performance evaluation of the SVC during the temporarily injected SLG fault is depicted in Figure 13. During the switching fault time from 0.02 to 0.06s, the reactive power (Q) is increased, making the system stable. Power quality is improved, and the supply continuity is maintained. The reactive power is generated by the SVC controller and reaches its optimized value. It can be observed that the proposed model generates a large amount of reactive power when the system voltage is low and achieves better performance in terms of voltage stability.

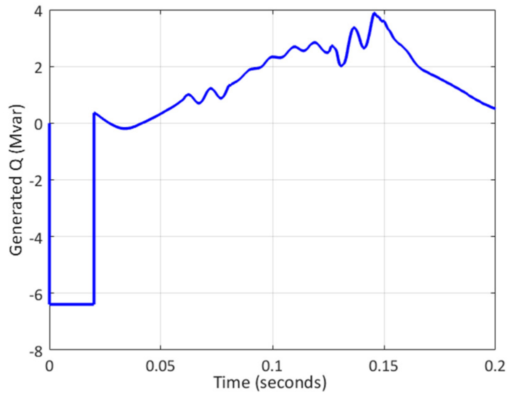

Fig. 13. Generated reactive power (Q) during SLG fault.

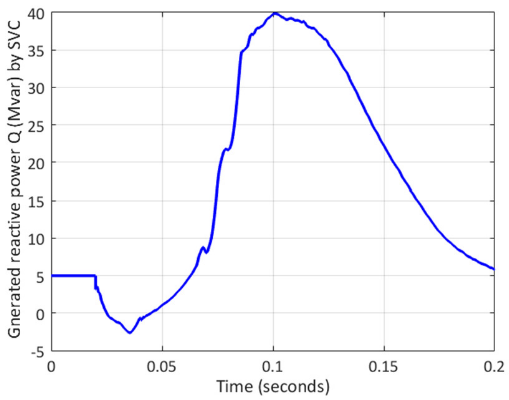

Fig. 14. Generated reactive power (Q) during SLG fault by the SVC.

C. System Response at Unsymmetrical L-L Fault

1) Without SVC

It can be seen in Figure 15 that two phases (red and blue phase) drop from 1.0 to 0.5p.u.. In Line to Line (L-L) fault, it is confirmed that the system is in severe condition which can make it stop from running. Figure 15 demonstrates the phase condition in which the system is disturbed, and the wind farm is tripped. Fault switching occurs between 0.03 and 0.13s. As per grid code requirements, the voltage dip should not fall below 0.75p.. Voltage dip is increased during the fault switching time. It can be noticed that the voltage sag produced by the L-L fault is more severe than the SLG fault. Furthermore, during the fault switching time, from 0.03 to 0.06s, the reactive power is decreased as shown in Figure 16.

2) With SVC

The static SVC controller is the key part of the proposed model. After the installation of SVC at PCC and during the fault period, voltage profile, voltage stability, and power quality are improved. It is also noticed that the voltage profile is improved from 0.45 to 0.75s as shown in Figure 17.

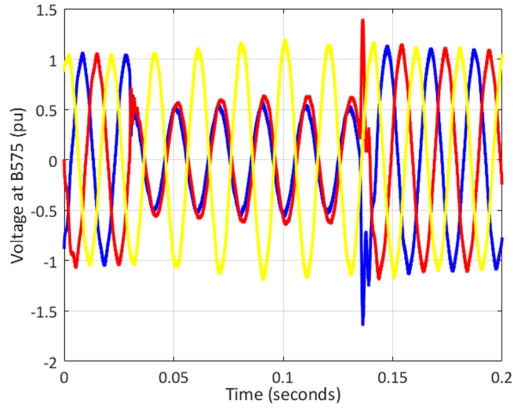

Fig. 15. Generated voltage at PCC during L-L fault.

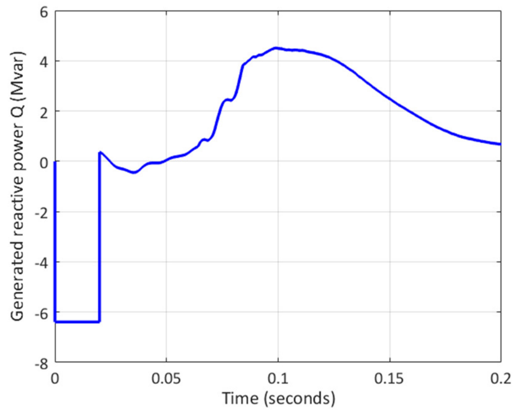

Fig. 16. Generated reactive power (Q) during L-L fault.

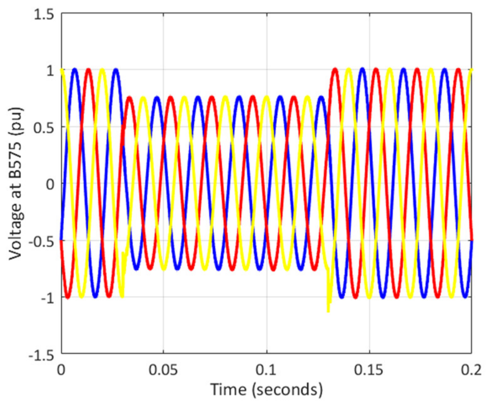

Fig. 17. Voltage at PCC during L-L fault with SVC.

Finally, it is confirmed that the simulation results show better performance in terms of power quality. The wind farm runs in a smooth way and continuity of supply is not disturbed. Figure 18 shows the optimized result of the proposed model. It is noted that SVC has generated a large amount of reactive power during the L-L fault. The proposed model shows enhanced performance and meets the required conditions. Further, it is observed that the model system is in operational condition and the supply remains uninterrupted.

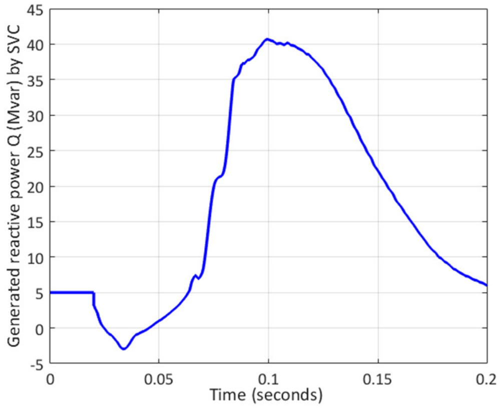

Fig. 18. Generated reactive power (Q) during L-L fault by the SVC.

IV. CONCLUSION

An LVRT enhancement of a grid-tied PMSG-based wind farm system has been proposed in this paper. It consists of 5 wind turbine generators integrated with the grid system. An LVRT control technique is implemented which has achieved balanced grid voltage. Reactive power is supplied during the fault condition to secure the protection of WECS of the wind turbine and as a result, it determines the enhanced LVRT capability. The proposed system has been designed with the use of the SVC controller. When a grid fault occurs, the SVC is automatically activated to regulate the grid voltage and compensate the power loss. The system model has been designed and simulated in MATLAB/Simulink. The simulation results reveal that the proposed system has superior performance in terms of power quality, voltage stability, and compensation of the reactive power in severe disturbances.

REFERENCES

[1] A. M. Howlader and T. Senjyu, "A comprehensive review of low voltage ride through capability strategies for the wind energy conversion systems," *Renewable and Sustainable Energy Reviews*, vol. 56, pp. 643–658, Apr. 2016, https://doi.org/10.1016/j.rser.2015.11.073.

[2] B. Khan and M. Kassas, "FSIG-Based Wind Power Plant Transient Stability Margin Improvement, a STATCOM/SVC Comparison," in *2019 IEEE Texas Power and Energy Conference (TPEC)*, College Station, TX, USA, Feb. 2019, https://doi.org/10.1109/TPEC.2019.8662129.

[3] M. Cheah-Mane, J. Liang, and N. Jenkins, "Permanent magnet synchronous generator for wind turbines: Modelling, control and Inertial Frequency Response," in *2014 49th International Universities Power Engineering Conference (UPEC)*, Cluj-Napoca, Romania, Sep. 2014, https://doi.org/10.1109/UPEC.2014.6934799.

[4] M. Hussain, M. H. Baloch, A. H. Memon, and N. K. Pathan, "Maximum Power Tracking System Based on Power Electronic Topology for Wind Energy Conversion System Applications," *Engineering, Technology & Applied Science Research*, vol. 8, no. 5, pp. 3392–3397, Oct. 2018, https://doi.org/10.48084/etasr.2251.

[5] M. Nasiri, J. Milimonfared, and S. H. Fathi, "A review of low-voltage ride-through enhancement methods for permanent magnet synchronous generator based wind turbines," *Renewable and Sustainable Energy Reviews*, vol. 47, pp. 399–415, Jul. 2015, https://doi.org/10.1016/j.rser.2015.03.079.

[6] Z. Memon, M. Uqaili, and M. Unar, "Design of Three-Phase Hybrid Active Power Filter for Compensating the Harmonic Currents of Three-Phase System," *Mehran University Research Journal of Engineering and Technology, Jamshoro, Pakistan*, vol. 31, no. 2, pp. 347–354, Apr. 2012.

[7] H. S. Dhiman and A. S. Deshpande, "Fault Ride-Through study of PMSG based offshore wind farms during grid faults," in *2016 IEEE 1st International Conference on Power Electronics, Intelligent Control and Energy Systems (ICPEICES)*, Delhi, India, Jul. 2016, https://doi.org/10.1109/ICPEICES.2016.7853258.

[8] X. Yang, X. Duan, F. Feng, and L. Tian, "Low Voltage Ride-Through of Directly Driven Wind Turbine with Permanent Magnet Synchronous Generator," in *2009 Asia-Pacific Power and Energy Engineering Conference*, Wuhan, China, Mar. 2009, https://doi.org/10.1109/APPEEC.2009.4918470.

[9] M. Nasiri, B. Faridpak, and M. Farrokhifar, "Low Voltage Ride Through Enhancement in PMSG-based Wind Turbines using De-loading Droop," in *2020 11th Power Electronics, Drive Systems, and Technologies Conference (PEDSTC)*, Tehran, Iran, Feb. 2020, https://doi.org/10.1109/PEDSTC49159.2020.9088374.

[10] I. A. Ethman, A. Yahfdhou, A. K. Mahmoud, and M. Maaroufi, "Statcom integration in a power grid to enhance voltage stability," *Indonesian Journal of Electrical Engineering and Informatics*, vol. 7, no. 4, pp. 620–627, Dec. 2019, https://doi.org/10.11591/ijeei.v7i4.990.

[11] S. H. Memon, M. Kumar, A. H. Memon, Z. A. Memon, and S. A. Soomro, "Total Harmonic Distortion (THD) Analysis of Grid Integrated Permanent Magnet Synchronous Generator (PMSG) With Full Scale Converter (FSC) Based Wind Farm," *International Journal of Computer Science and Network Security*, vol. 18, no. 12, pp. 232–238, Dec. 2018.

[12] S. L. S. Louarem, D. E. C. Belkhiat, T. Bouktir, and S. Belkhiat, "An Efficient Active and Reactive Power Control of DFIG for a Wind Power Generator," *Engineering, Technology & Applied Science Research*, vol. 9, no. 5, pp. 4775–4782, Oct. 2019, https://doi.org/10.48084/etasr.3007.

[13] T. Ahmed, M. H. Baloch, N. Khan, G. Mehr, B. A. Mirjat, and Y. A. Memon, "Experimental Analysis and Control of a Wind-Generator System through a DC-DC Boost Converter for Extremum Seeking," *Engineering, Technology & Applied Science Research*, vol. 11, no. 1, pp. 6714–6718, Feb. 2021, https://doi.org/10.48084/etasr.3948.

[14] S. H. Memon, Z. A. Memon, M. A. Uqaili, and Shan-E-Farooq, "Voltage Stability and Reactive Power Compensation of 132kv Grid Integrated 50MW Wind Farm Using Statcom," *Journal of Applied Environmental and Biological Sciences*, vol. 8, no. 1, pp. 232–240, 2018.

[15] L. Sartika, M. Rosyadi, A. Umemura, R. Takahashi, and J. Tamura, "Cooperated stabilizing control of PMSG based grid connected wind farm," in *2015 IEEE Energy Conversion Congress and Exposition (ECCE)*, Montreal, Canada, Sep. 2015, pp. 3482–3488, https://doi.org/10.1109/ECCE.2015.7310152.

[16] M. Nasiri, S. Mobayen, and Q. M. Zhu, "Super-Twisting Sliding Mode Control for Gearless PMSG-Based Wind Turbine," *Complexity*, vol. 2019, Apr. 2019, Art. no. e6141607, https://doi.org/10.1155/2019/6141607.

[17] A. Mahrouch, M. Ouassaid, and K. Elyaalaoui, "LVRT Control for Wind Farm Based on Permanent Magnet Synchronous Generator Connected into the Grid," in *2017 International Renewable and Sustainable Energy Conference (IRSEC)*, Tangier, Morocco, Dec. 2017, https://doi.org/10.1109/IRSEC.2017.8477281.

[18] M. I. Hossain and M. A. Abido, "Positive-Negative Sequence Current Controller for LVRT Improvement of Wind Farms Integrated MMC-HVDC Network," *IEEE Access*, vol. 8, pp. 193314–193339, 2020, https://doi.org/10.1109/ACCESS.2020.3032400.

[19] V. F. Mendes, F. F. Matos, S. Y. Liu, A. F. Cupertino, H. A. Pereira, and C. V. De Sousa, "Low Voltage Ride-Through Capability Solutions for Permanent Magnet Synchronous Wind Generators," *Energies*, vol. 9, no. 1, Jan. 2016, Art. no. 59, https://doi.org/10.3390/en9010059.